Mykola Malashevskyi[1], Olena Malashevska[2]

Advanced Method
for Determining Land Plot's Physical Surface

Abstract: This study examines the issue of the accuracy of physical surface calculations for land plots with complex configurations and reliefs. The goal of the study was to develop a methodology for determining the surface area of land plots with complex configurations and reliefs. The presented model was based on the finite element method. The developed method allows one to evaluate a relief's complexity by using a dimensionless mean physical surface complexity factor; a Fortran program was developed for the methodology. Experiments that proved the effectiveness of the methodology and a comparative analysis of those areas that were calculated by the presented method and TIN model were carried out. The research findings proved the practicability of the methodology for calculating the physical surfaces of land plots with complex configurations. The presented methodology can be used for flood modeling, landscape and vertical planning, etc.

Keywords: DEM, area measurement, finite element method, TIN model, GRID model

[1] The Institute of Land Management of National Academy of Agrarian Sciences of Ukraine, Department of Problems of Land Development and Land Cadastre, Kyiv, Ukraine, email: mykola.malashevskyi@gmail.com, https://orcid.org/0000-0001-7171-8835
[2] National University of Life and Environmental Sciences of Ukraine, Geodesy and Cartography Department, Kyiv, Ukraine, email: olenamalashevska@gmail.com (corresponding author), https://orcid.org/0000-0002-5387-5674

1. Introduction

With the development of measuring equipment, computers, and data processing, the demands on the accuracy of land plot area determinations are constantly increasing [1]. According to the World Bank, natural resource management, agricultural productivity, well-being, etc. depend on the accuracy of land area determinations: "Analyses of wealth and inequality, agrarian structures, agricultural yields and productivity, natural resource management, and gender differentials in agriculture all depend on accurate measures of land areas" [2].

An area is usually calculated with the help of an analytical method that uses its land plot boundary coordinates [3]. Generally, the area is calculated by actual measurements and cartographical materials [4] as well as with satellite images [5]. The development of area-determination methods is based on global positioning systems, laser scanning, earth remote sensing, and advanced geoinformational technologies. With technological advancements, the improvement of analytical area-determination methods is an urgent task.

The physical characteristics of relief are among the factors that influence the accuracy of area determination; therefore, determining the areas of the physical surfaces of land plots is an urgent issue.

Land plot area determination that considers a physical surface is especially important for tasks like earthwork calculation [6, 7], environmental monitoring, civic plan subsystems, traffic subsystems, electric power subsystem planning [8], flood modeling [9], hydraulic erosion modeling [10], and engineering and geological modeling [11].

A digital relief model is needed to calculate an area by considering its relief. Wilson and Gallant [12] carried out the detailed of digital elevation model (DEM) development methods. Generally, DEM was developed as a triangulated irregular network (TIN) and regular grid-based DEM [13]. TIN and GRID models are relatively easy to develop in the GIS environment [14]. Spline-based techniques for developing multi-resolution terrain models are widespread [15, 16]. Considerable attention has been paid to the issue of interpolation for the development of land-surface models [17].

The choice of an approach to the development of DEM depends on a set of factors, which include topographical conditions, the goals of DEM, the source data type, the way it was collected, etc. It predefines the existence of various approaches toward improving the TIN and GRID models.

DEM can be developed from various data types to include photogrammetric, surveying, the global positioning system (GPS), and light detection and ranging data (LiDAR) [18, 19]. Most algorithms utilize either a dense digital elevation model (DEM) or a set of digitized outlines as their input data [20]. The development of DEM from data that is obtained by aerial laser scanning is of considerable interest. A TIN model can be developed from a selection of points from a LiDAR point cloud [20]; a regular elevation grid can then be developed.

TIN is the most widespread digital-elevation model [21]; for example, TIN-constrained Delaunay triangular irregular network modeling is also extensively used [22]. There are various approaches for improving the TIN model; improving the TIN model with the Delaunay condition [9] by adding or using breaklines or manual additional points [21] has been extensively scrutinized. The TIN vertex-based method has been compared with the TIN facet-based method for calculating slope and aspect [22]. In order to substantiate the distortion of DEM that has been developed by traditional methods for discontinuous terrains (roads and building foundations), the development of a TIN model by combining the topographic feature line and other available topographic data was suggested for its construction [23]. The compound method of DEM generalization by retrieving significant points from a grid DEM to generate a TIN surface was examined [24].

There are a number of approaches for improving the GRID model (for example, by embedded terrain features [25]) or developing a grid DEM that is based on a Coons surface [17].

In order to provide the necessary accuracy of an area determination, the geometrical characteristics of a land plot should be considered to be on a par with the relief topography. In the case when the area of a land plot is determined as a plane polygon with the help of GPS/EGNOS, any calculation mistakes do not depend on the form of the land plot [26]; however, the configuration influences the accuracy of the area determination when calculating the area while considering its relief. Traditional methods of area determination have proven to be ineffective in this case.

The working hypothesis is that determining the land plot areas of complex configurations by traditional methods fails to fully consider the physical surfaces of the terrains. There is a need for the development of advanced methodologies to address land plots of various outlines and consider their reliefs. At the current stage, there is no unified approach to the accurate physical surface determination of land plots with complex configurations that is sufficient for modern territory management. This is why there are a number of approaches for improving DEM and 3D modeling. The goal is to develop a land-plot physical-surface-determination method that would not require a labor-intensive topographic survey. The use of a regular elevation grid is suggested. The implementation of the finite element method and the development of Fortran software will increase the accuracy of area determinations and introduce a uniform system.

The goal of the research is to develop a land-plot area-determination methodology that considering a terrain's physical surface.

2. Materials and Methods

The main geometrical task of the study was to determine the surface areas of land plots with complex configurations considering their reliefs. In order to do this, a set of key steps were performed; these are presented in Figure 1.
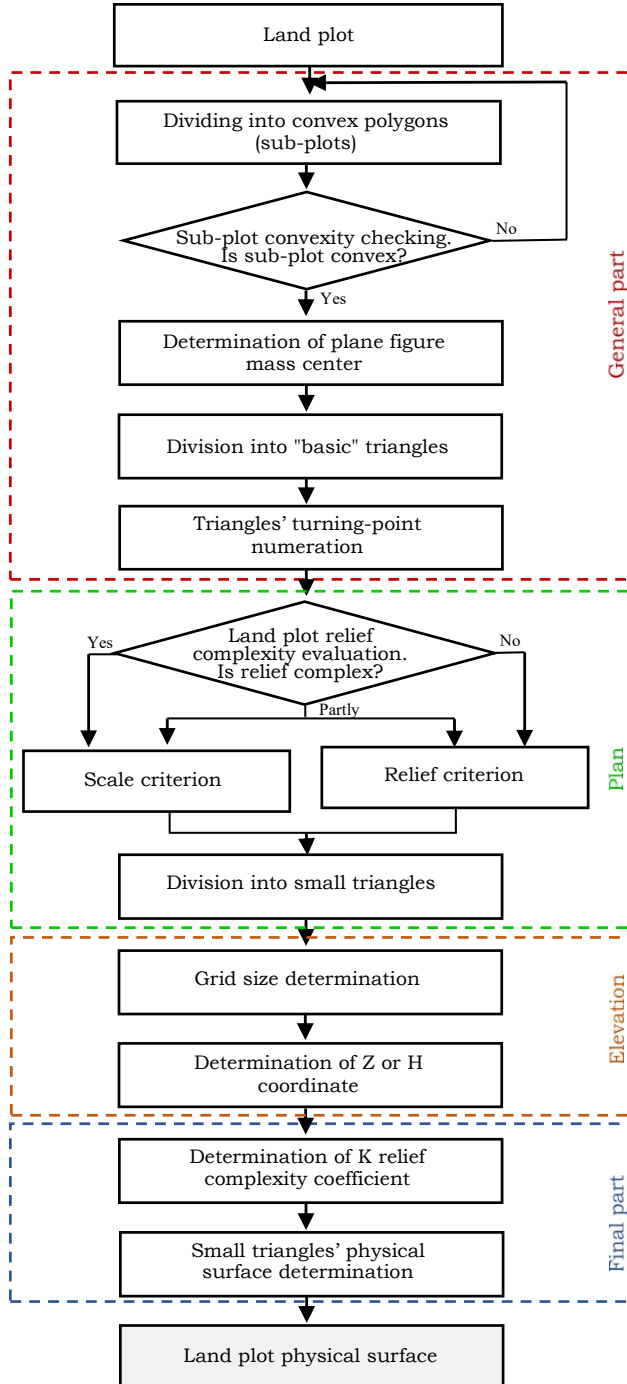
Fig. 1. Key stages of determining land plot's physical surface

In the first stage, the configuration of the land plot is considered. Determining the area can be carried out for any configuration; for example, the stretched-out or branched-off parts of the land plot (Fig. 2). At this stage, the land plot is divided into a number of sub-plots. The implementation of the finite element procedure is suggested [27–29] by the division of the land plot into a number of convex polygons and their subsequent divisions into triangles.
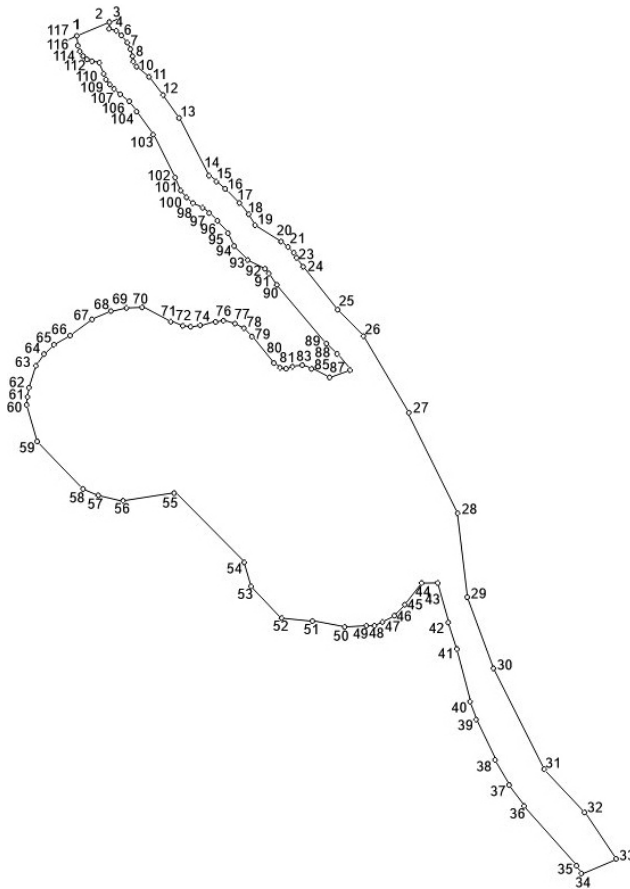

Fig. 2. Irregularly shaped polygon

The computer-aided division of an irregular land plot is not practical; a methodology for an automated sub-plot convexity check is suggested for this step.

In the second stage, each sub-plot is divided into a set of "basic" triangles. The plane figure's mass center is used for the subsequent divisions of the sub-plot into triangles. As is known from physics, the mass center of a regular geometric figure is the symmetry center of this figure. If a regular figure is convex, its mass center is situated at the same distance from each apex.

When the mass center is determined, each sub-plot is divided into so-called "basic" triangles, with each of their apexes in the mass centers and the polygon segments between two successive turning points as their bases.

It is the division of sub-plots into "basic" triangles with their apexes in their mass centers that predefines the need for the division into convex sub-plots at the previous stage.

If we divide each side of the basic triangle by the same number of equal segments, the basic triangle will be divided into a number of identical triangles (similar to the basic triangle). The more segments that the side of the triangle is divided into, the smaller are the triangles; thus, the higher is the accuracy of the area determination.

For example, each side of a triangle is divided into four segments in Figure 3; straight lines are drawn between the respective points on the sides that are parallel to the base, then straight lines are drawn between the respective points of one side and the base that is parallel to the other side. The third group of parallel lines is drawn the same manner. Thus, the initial triangle is divided into a number of identical triangles (which are similar to the basic triangle). In the case when the initial triangle is close to the regular triangle, the triangles that were developed from the initial triangle are close to regular triangles.

There is a need for automated turning-point numeration after the division. The developed approach to the numeration of the triangle's turning points is presented in Figure 4.
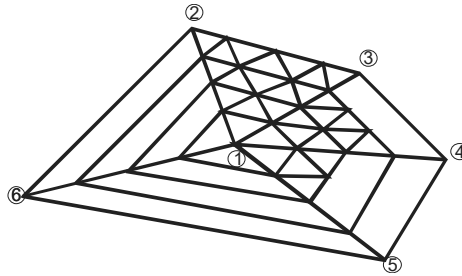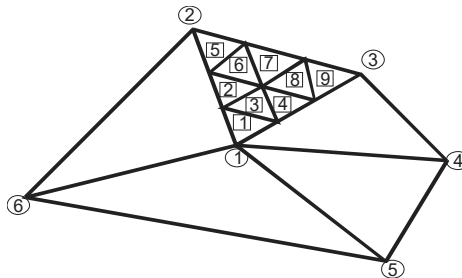

Fig. 3. Division pattern

Fig. 4. Triangle turning-point-numeration pattern

Based on the suggested approach to the numeration, the automated triangle turning-point-numeration method is presented in Figure 5.
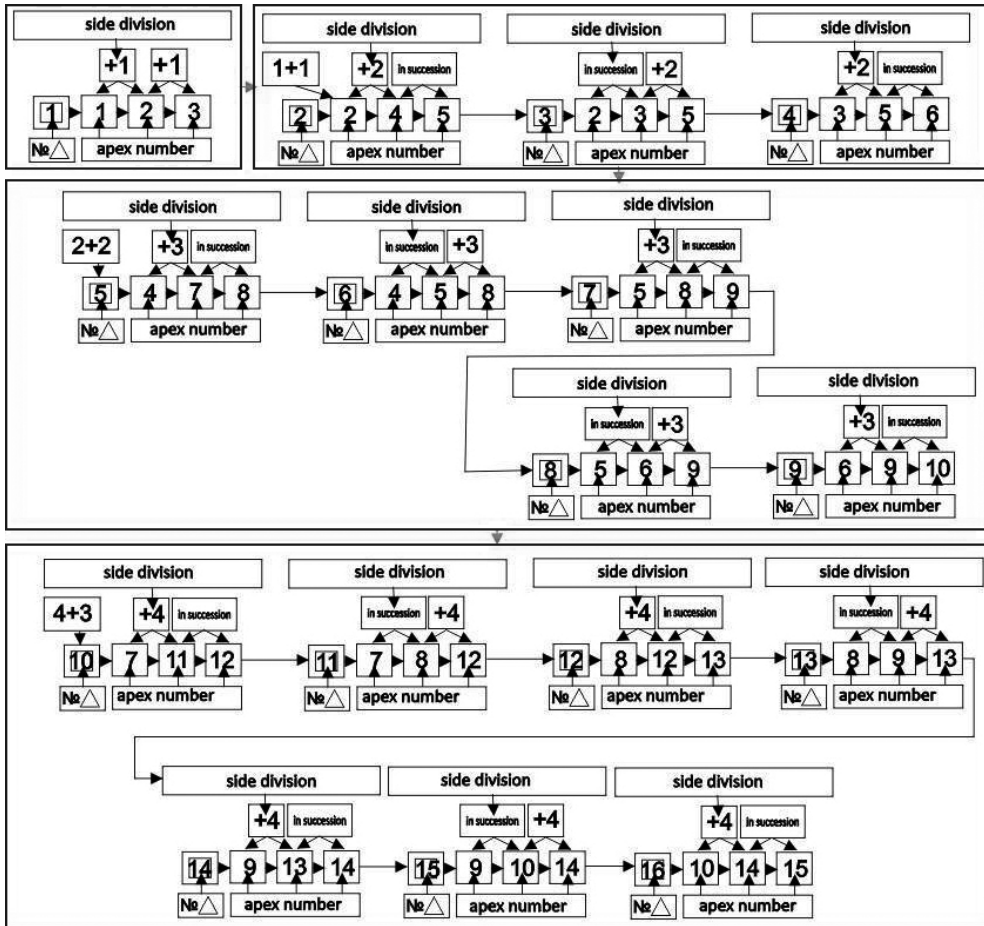

Fig. 5. Triangle turning-point-numeration method

The mass center of the plot is connected to each subsequent pair of turning points (by number), beginning with the lowest number. The numeration starts from the mass center and proceeds in a counter-clockwise manner. The algorithm was developed so that the number of a triangle can be clearly defined by the numbers of apexes. Figure 6 illustrates that the number of each triangle can be defined by subtracting the number of the mass center (number one in this picture) from the number of the apex.

Such an approach to the apex numeration simplifies the algorithm and provides the identification of each triangle for the area determination in the following stages; the reason for this is that the area is calculated for each triangle separately.
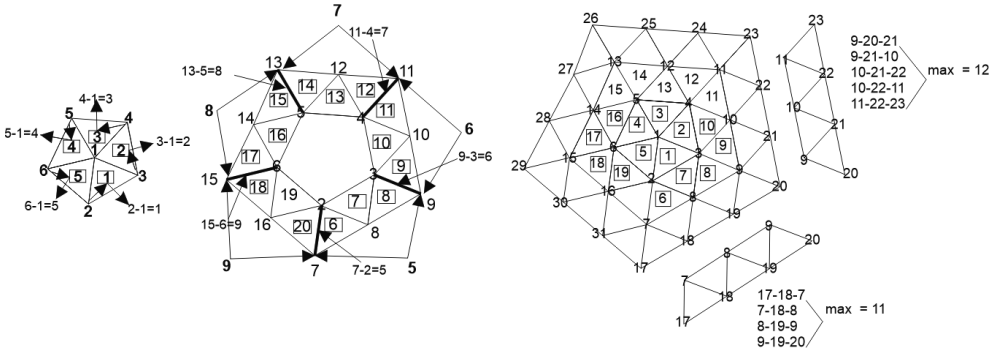
Fig. 6. Triangle-numeration pattern by turning-point numeration

The above-mentioned identification pattern for the mass centers, sides, and triangles is the basis for the development of the area-determination algorithm. This does not depend on the quantity of elements into which the sub-plot is divided.

In the third stage, the area is calculated with an accuracy that is predefined by the relief. The area to be determined is basically the area of the complicated irregular surface; therefore, the surface is to be approximated by some standard surfaces. A flat triangle is the simplest and, at the same time, a very accurate example of such a standard surface. As mentioned above, each of these triangles is further divided into a set of smaller triangles in order to increase the accuracy of the area determination considering the relief. The elevation of the smaller triangle's apex is defined by its coordinates using a digital map, and the area of the triangle (inclined to the horizontal plane) is calculated by analytical geometry formulas.

The total area of the plot that considers its relief is calculated as the sum of all of the smaller inclined triangles. It has been suggested to evaluate the relief with coefficient $0 < K \leq 1$. The lower the value of K, the more complicated the relief of the land plot is. In the case when coefficient K is close to one, relief may not be considered. Thus, the presented method allows us to automatically define the mean inclination of a land plot. A separate smaller triangle is presented in Figure 7.
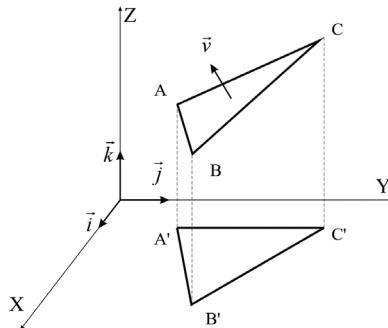

Fig. 7. Triangle inclination toward horizontal plane

For such a small triangle, the angle cosine between the vertical axis and the triangle plane is determined by the normal v. The small triangle plane equation that is determined by the coordinates of its apexes is as follows:

$$\begin{vmatrix} x-x_A & y-y_A & z-z_A \\ x_B-x_A & y_B-y_A & z_B-z_A \\ x_C-x_A & y_C-y_A & z_C-z_A \end{vmatrix} = 0 \tag{1}$$

The normal vector to the triangle plane is as follows:

$$\vec{N} = N_x\vec{i} + N_y\vec{j} + N_z\vec{k} \tag{2}$$

where:

$$N_x = \begin{vmatrix} y_B-y_A & z_B-z_A \\ y_C-y_A & z_C-z_A \end{vmatrix} \tag{3}$$

$$N_y = \begin{vmatrix} x_B-x_A & z_B-z_A \\ x_C-x_A & z_C-z_A \end{vmatrix} \tag{4}$$

$$N_z = \begin{vmatrix} x_B-x_A & y_B-y_A \\ x_C-x_A & y_C-y_A \end{vmatrix} \tag{5}$$

The angle cosine between the vertical axis and the normal of the triangle plane is determined by the following formula:

$$c_i = \cos(\vec{N}, \vec{k}) = \frac{N_z}{\sqrt{N_x^2 + N_y^2 + N_z^2}} \tag{6}$$

If F_i^* is the area of a solid triangle and F_i is the area of its floor projection, then:

$$F_i^* = \frac{F_i}{\cos(\vec{N}, \vec{k})} \tag{7}$$

then, for one triangle:

$$c_i = \frac{F_i}{F_i^*} \tag{8}$$

As far as the area of the polygon is the total of all of the triangles into which the polygon has been divided, angle cosine weighted mean value c_{av} is calculated by the following formula:

$$c_{av} = \frac{\sum c_i F_i}{\sum F_i} = K \tag{9}$$

where F_i is the floor-projection area of the i-th triangle.

In this case, the introduced coefficient is the ratio of the floor-projection area to the area that considers the relief. Generally, it can be stated that coefficient *K* characterizes the averaged ratio of the floor-projection area to the area that considers the relief.

The fourth stage is determining the vertical coordinates of the plot points. This stage begins with applying the orthogonal grid to the plot (Fig. 8). The suggested method is based on the GRID model.
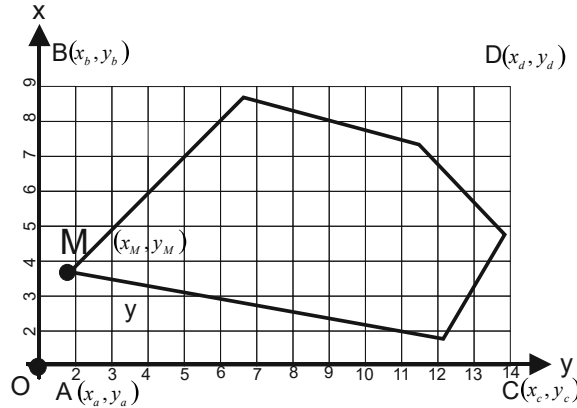

Fig. 8. Defining elevation of land plot turning points

The elevation in the grid nodes is defined; these values form rectangular matrix *m* × *n* in the algorithm. The matrix row number is predefined by the sequence number of the grid node by the *x* coordinate, and the matrix column number is predefined by the grid node number by the *y* coordinate. The coordinates of the four turning points (*A*, *B*, *C*, and *D*) are determined in the polygon.

The grid size is set depending on the required accuracy and relief complexity ($\Delta_X = \Delta_Y = \Delta$). In the case of a complicated relief, an increased quantity of grid nodes is necessary [30]. The smaller is the grid size, the more accurate the determination of the elevation is. It is not reasonable to decrease the grid size to the graphical accuracy of the scale and 1/3 of the vertical distance between the counter lines; a grid size of 5 m × 5 m to 20 m × 20 m is recommended [31]. The example of the algorithm output for $\Delta = 10$ mm in the cartographic base scale is presented in the study.

The number of the lower-left point of the grid cell under consideration is determined by the following formulas:

$$m = E\left(\frac{x_D - x_A}{\Delta} \right) \tag{10}$$

$$n = E\left(\frac{y_B - y_A}{\Delta} \right) \tag{11}$$

where $E(x)$ is the integer part of the *x* value, and $E(y)$ is the integer part of the *y* value.

The plot area that considers the relief is calculated as the total area of all of the small triangles. For each triangle apex, two horizontal coordinates are determined; the third coordinate (i.e., elevation) is determined with the help of a digital map.

3. Results

A Fortran-4 program has been developed for the methodology. Fortran programs have proven their effectiveness for calculations based on the finite element method and are extensively used in civil engineering [32].

The area-calculation algorithm is presented in Figure 9; a Fortran syntax was used.
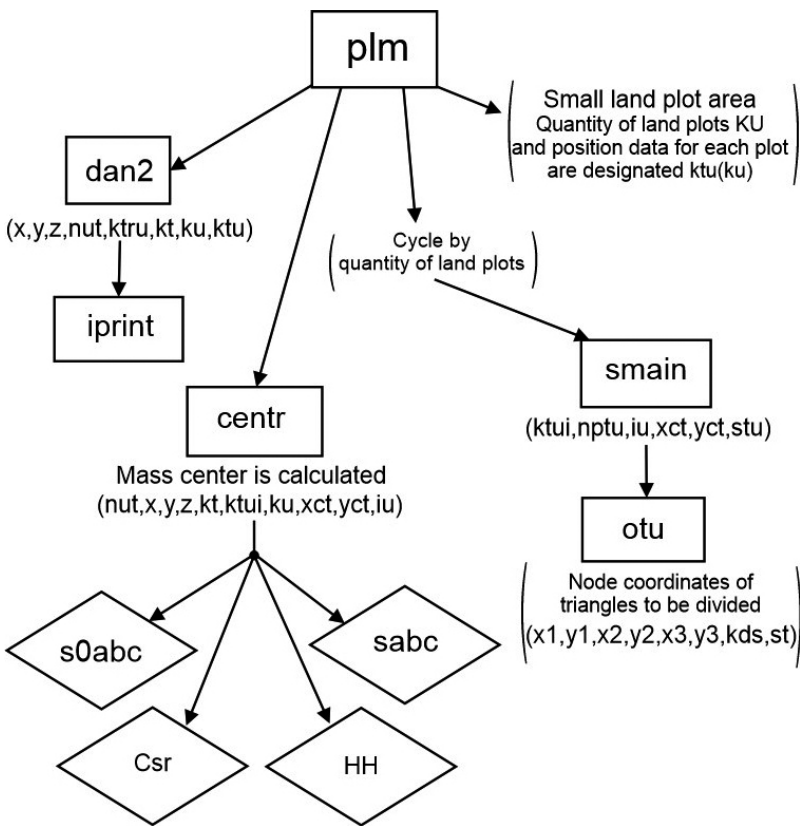
Fig. 9. Fortran area-determination algorithm

All of the variables that are used in the program are divided into simple variables and arrays; they are declared by respective names in the language. The following names (Table 1) are declared for the key variables.

Table 1. Names that are used in algorithm

Gist of variable	Name	Variable type
Polygon turning-point quantity	n	simple variable
Triangle-node number	nut (3400, ku)	3D array
Quantity of triangles in sub-plot	ktru (ku)	array
Plot-node number	ntu (2000)	array
Polygon turning-point-total quantity	ktu	simple variable
Triangle-node quantity	kut	simple variable
Big triangle side-division-point quantity	kds	simple variable
Triangle-node quantity	kt	simple variable
Big triangle side-division-point quantity	kds	array
Triangle-node quantity	ktu	simple variable
Triangle-shaped plot-node number	nttu (1000)	simple variable
Plot-last-point number	nptu	simple variable
Current sub-plot center coordinates	xct, yct	simple variable
Current sub-plot point quantity	ktui	simple variable
Quantity of sub-plots into which polygon is divided	ku	simple variable
Last triangle-node number	nupt (3, 1000)	array
Plot-node quantity	kuu	simple variable
Plot quantity	su	simple variable
Current node number	iu	simple variable

For the area calculations of land plots with complicated outlines and reliefs, it has been revealed that, with the increased division iterations, there arises an effect that is similar to the fractal effect. In order to prevent endless division, the criteria of the cartographic base scale and elevation have been introduced.

The graphical accuracy of the point-determination scale in the cartographic materials (which is $m' = 0.2$ mm in the cartographic base scale) is the first criterion that outlines the least-recommended range. The second criterion is the mean error of the relief survey toward the nearby points, which is 1/3 h. This value should not exceed the difference between the vertical coordinates of the two nearby points of a triangle.

As the result of the examination, it has been suggested that the criterion of the map scale be applied to land plots with complicated reliefs, and the criterion of relief

is used for those areas of plain relief. In the case when the land plot is partly of complicated relief and partly of plain relief, both criteria are automatically implemented at the same time.

Let us scrutinize an example of the area calculation for a land plot with complicated outlines and a complicated relief using the developed method. The calculations of the area for the land plot with the complicated outlines are presented in Table 2 (map scale – 1:2,000).

Table 2. Complicated outline land plot area calculation (1:2,000)

Land plot-side division	Land plot floor-projection area [m²] (x, y)	Land plot area considering relief (physical area), [m²] (x, y, z) $H = 0.5$	Relief-complicatedness coefficient $H = 0.5$	Difference between physical area and floor-projection area [%] $H = 0.5$	Triangle side length [m]
1	846,668	849,380	0.99	0.3	34.300
2	846,668	855,391	0.97	1.0	14.710
3	846,668	864,706	0.95	2.1	11.430
4	846,668	873,160	0.94	3.1	8.575
5	846,668	881,678	0.92	4.1	6.860
6	846,668	886,299	0.91	4.6	5.717
7	846,668	891,111	0.90	5.2	4.900
8	846,668	895,038	0.89	5.7	4.288
9	846,668	899,246	0.89	6.2	3.811
10	846,668	902,881	0.88	6.6	3.430
15	846,668	911,370	0.87	7.6	2.287
20	846,668	921,107	0.85	8.7	1.715
25	846,668	929,198	0.84	9.7	1.372
30	846,668	936,481	0.84	10.6	1.143
31	846,668	936,481	0.84	10.6	1.143

Table 2 illustrates how the area of the land plot considers the relief changes depending on the side-division quantity. With increases in the side divisions, the area is increased since the relief is considered more precisely. The refinement of the physical area with the increases in the side divisions is illustrated in Figure 10.
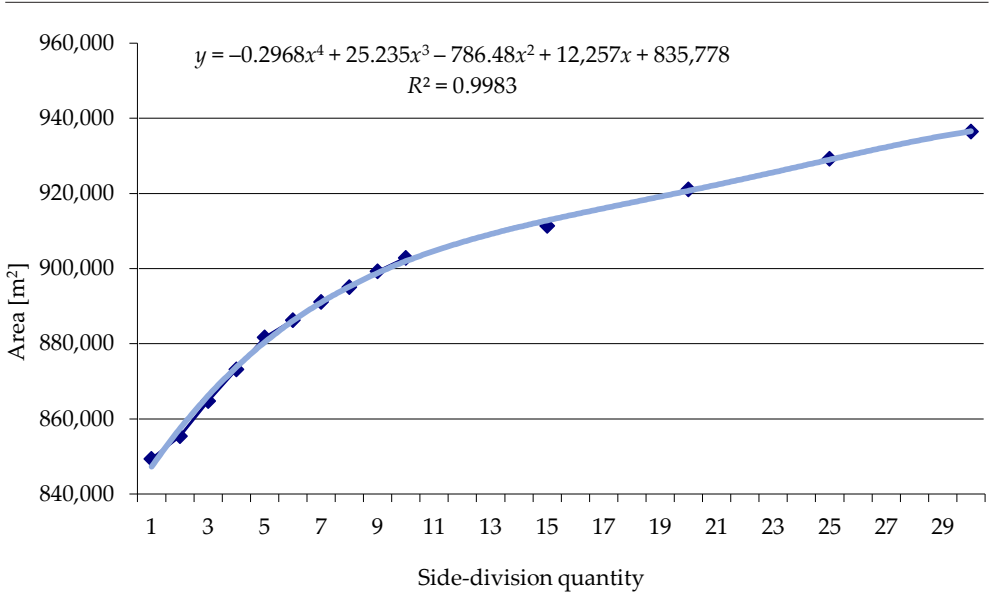
$$y = -0.2968x^4 + 25.235x^3 - 786.48x^2 + 12{,}257x + 835{,}778$$
$$R^2 = 0.9983$$

Fig. 10. Land plot area determination (scale – 1:2,000)

The algorithm stopped the division at the 30th iteration due to the scale criterion (in this case, $m' = 0.4$ m). The data that is presented in Table 2 on the 31st iteration corroborated the practicability of the limitation. The approach corresponded with the iteration process in general [33]. More iterations are not rational for the prescribed accuracy of area determination; the area of the land plot is 936,481 m² at a scale of 1:2,000. This value differed by 10.6% from the area that was determined without considering the physical area.

The summary data on the land plot area determination for various scales is presented in Table 3.

Table 3. Complicated configuration land plot area determination for various scales

Scale	Land plot floor projection area [m²] (x, y)	Land plot area considering relief (physical area) [m²] (x, y, z)	Relief complicatedness coefficient $H = 0.5$	Land plot side division	Difference of physical area and floor projection area [%] $H = 0.5$
1:10,000	846,668	875,015	0.92	5	4.5
1:5,000	846,668	907,605	0.89	10	7.1
1:2,000	846,668	936,481	0.84	30	10.6
1:1,000	846,668	937,262	0.83	32	10.5
1:500	846,668	956,730	0.82	33	11.3

Based on the developed program, the comparative analysis of the land plot physical area determination was carried out using the TIN and GRID models.

Fig. 11. Land plot physical area modeling using TIN model

In Figure 11, an irregular polygon with a set of stakes is presented; based on this, an irregular grid was developed (TIN model).

Fig. 12. Territory GRID model fragment

In Figure 12, an irregular polygon with a set of stakes is presented; based on this, a regular grid was developed (GRID model). Digital elevation models can be developed automatically with the help of a digital photogrammetric station [34].

With the help of the developed method of the irregular polygon determination, five convex sub-plots were developed automatically (Fig. 13). Each sub-plot

was automatically divided into *n* triangles using the criteria of the graphical accuracy of the point determination in maps and plans and the mean error of the relief survey toward the nearby points. This was the way the set of regular triangles was developed.

The physical area of the irregular polygon was 183,910 m² by the developed methodology.

Fig. 13. Land plot physical surface modeling by developed methodology

Table 4. Physical area calculation comparative analysis

Area calculation options	Calculated area [m²]	Reference area by TIN model [m²]	Deviation from reference area [m²]	Deviation from reference area [%]
Without relief consideration	846,668	940,737	−94,069	−10.0
By developed methodology	956,730	940,737	159,930	+1.7

A comparative analysis of the physical area calculation using the reference TIN model and the developed methodology is presented in Table 4.

Thus, the presented methodology allowed us to increase the accuracy of the land plot area calculation by 110,062 m² as compared to the area calculation without considering the relief. The area that was calculated by the presented methodology was more accurate than the area that was determined by the TIN model.

4. Discussion

The research findings and their practical implementations upheld the working hypothesis: the presented algorithm allows us to determine the area of a land plot with a complex configuration more accurately. For the presented example, the area was increased by 1.7 and 11.7% due to the advanced calculation method as compared to the TIN model and the calculation without considering the physical surface, respectively. These figures are significant – especially for land plots with high market prices. Accurate area determination is important for landscape design, fertilizer distribution, erosion modeling, avalanche/mudslide/rock slide forecasting, ski resort management, construction site vertical planning, etc. [35].

With the increased accuracy of the data based on relief, the better quality of development projects and increased productivity can be observed [7]; the modeling can be an alternative to 3D modeling. The difference of the actual relief from the design values by the existing methods is a reason for extra costs and time expenditures due to the extra earth excavation [36].

Generally, the abovementioned is about projects that demand precise determinations of area and are related to area calculations (like volume) for large terrains with complicated reliefs. First of all, natural disasters should be considered [35]; i.e., floods, rock slides, snow avalanches, etc. In such cases, the accurate determination of area and, respectively, the volume decreases time and resource consumption, facilitates search-and-rescue operations, and aids in rehabilitating a territory.

At the current stage, unmanned aerial vehicles are used to develop accurate DEMs [36]. The presented method allows us to model relief and determine area and, respectively, volume based on existing cartographic materials. The technique is more cost-effective than those that use unmanned aerial vehicles. The advantages of developing DEM from topographic maps were corroborated by the research findings [37].

The study can be considered for the purpose of determining the impact of area-calculation accuracy on agricultural productivity [38] or determining the actual area of a farm [39].

The algorithm is based on the GRID model and has all of its advantages (including simplicity). At the same time, the presented algorithm allows us to avoid the disadvantages of the GRID model [13]. Due to the development of a set of regular triangles, drastic elevation differences and detailed relief patterns on plain areas can be reflected. At the same time, we agree on the practicability of improving the collection of significant points for the formations of grid-based DEMs [40]. Considering the abovementioned, the adjustment of the approach to the selection of LiDAR points [20] to the presented method is promising, and adjusting the approach to determining the thresholds of the input density of points that are detected by LiDAR is possible [41].

Regular triangles are used for the presented algorithm. The triangle-formation method for the surface approximation is also important for TIN models. Delaunay triangulation [42, 43] allows us to maximize the inside angles of the triangles. The presented method provides for the development of regular triangles, which allows us to increase the accuracy of land plot area determination for land plots with complicated reliefs and configurations. The inclination of each regular triangle into which the surface is divided is considered; thus, the accuracy of the orthogonal projection on the plane is increased. The quantity of the divisions can be corrected according to reference conditions. The numeration of triangles of any type is considered by the presented methodology irrespective of the quantity of the divisions. The quantity of the divisions is limited by the practicability of the area specification considering any topographical survey errors and point positioning on a cartographic document. With the alteration of the requirements, the quantity of the divisions can be easily adjusted and the accuracy of the area determination improved.

As compared to the existing finite element model [28], the presented model allows us to distinguish plains from steep areas.

5. Conclusion

The developed methodology allows us to increase the quality of relief physical surface modeling and, as the result, increase the accuracy of physical area determinations for land plots with complicated outlines. The DEM is developed as a set of regular triangles. The method of determining the relief-complexity coefficient based on the finite element method was presented for the first time. Implementing the coefficient allowed us to determine the area of the physical surface of a land plot more accurately as compared to the existing methods. The effectiveness of the model was approved in practice and contrasted with the area that was determined by the TIN model.

The developed methodology allows us to do the following:
– decrease risks of mistakes when determining land plot areas,
– automate process of determining irregular land plot areas by analytical methods.

The method is practicable for projects that require determining areas and related calculations (like volume) for large and complex terrains; i.e., those that deal with vertical planning, floods, stone landslides, snow avalanches, etc. The method is practicable for decision-making on labor efforts and equipment utilizations for emergency interventions, earthworks, etc.

Funding

This research received no specific grant from any funding agency in the public, commercial, and not-for-profit sectors.

CRediT Author Contribution

M. M.: conceptualization, methodology, software, image processing, validation, resources, visualization, writing – review and editing, supervision, project administration.

O. M.: validation, formal analysis, investigation, data curation, writing – original draft preparation, visualization.

Declaration of Competing Interest

The authors declare that they have no known competing financial interests or personal relationships that could have appeared to influence the work that was reported in this paper.

Data Availability

The original contributions that were presented in the study are included in the article; further inquiries can be directed to the corresponding authors.

Use of Generative AI and AI-assisted Technologies

No generative AI or AI-assisted technologies were employed in the preparation of this manuscript.

References

[1] Windarni V.A., Sediyono E., Setiawan A.: *The evaluation of land area measurement using GPS technology*. Jurnal Ilmiah Kursor, vol. 9(1), 2017, pp. 1–8. https://doi.org/10.28961/kursor.v9i1.120.

[2] Carletto G., Gourlay S., Murray S., Zezza A.: *Land Area Measurement in Household Surveys: A Guidebook*. World Bank, Washington DC, 2016.

[3] Sandeep K.: *GPS based handheld system for land area measurement*. International Journal for Research in Applied Science & Engineering Technology, vol. 9, 2021, pp. 1619–1624. https://doi.org/10.22214/ijraset.2021.35302.

[4] FAO: *FAO Training Series. 10. Measurement of Areas*. https://www.fao.org/fishery/static/FAO_Training/FAO_Training/General/x6707e/x6707e10.htm [access: 30.03.2023].

[5] Kumar L.A., Jebarani M.R.E., Krishnan V.G., Ahmad M.W.: *Multitemporal change detection and irregular land shape area measurement from multispectral sensor images through BSO algorithm*. Mathematical Problems in Engineering, 2022, 3090074. https://doi.org/10.1155/2022/3090074.

[6] Hao X., Pan Yu.: *Accuracy analysis of earthwork calculation based on triangulated irregular network (TIN)*. Intelligent Automation & Soft Computing, vol. 17(6), 2011, pp. 793–802. https://doi.org/10.1080/10798587.2011.10643188.

[7] Kim J., Kim H., Tanoli W., Seo J.: *3D earthwork BIM design and its application in an advanced construction equipment operation*. Architecture and Engineering, vol. 4(2), 2019, pp. 22–26. https://doi.org/10.23968/2500-0055-2019-4-2-22-26.

[8] Nguyen V.T.: *Building TIN (triangular irregular network) problem in topology model*. [in:] *2010 International Conference on Machine Learning and Cybernetics (ICMLC 2010), 11–14 July 2010, Qingdao, China*, vol. 1, IEEE, Piscataway 2010, pp. 14–21. https://doi.org/10.1109/ICMLC.2010.5581100.

[9] Li Z., Wu L., Zhang Z., Yang Y.: *CD-TIN based urban inundation simulation method and its experiment*. Geomatics and Information Science of Wuhan University, vol. 39(9), 2014, pp. 1080–1085. https://doi.org/10.13203/j.whugis20120098.

[10] Skorkovská V., Kolingerova I., Benes B.: *Hydraulic erosion modeling on a triangular mesh*. [in:] Růžičková K., Inspektor T. (eds.), *Surface Models for Geosciences*, Lecture Notes in Geoinformation and Cartography, Springer, Cham 2015, pp. 237–247. https://doi.org/10.1007/978-3-319-18407-4_20.

[11] He L., Li X., Lei S., Bi B., Chen S.: *A front advancing adaptive triangular mesh dynamic generation algorithm and its application in 3D geological modeling*. Sustainability, vol. 15(9), 2023, 7214. https://doi.org/10.3390/su15097214.

[12] Wilson J.P., Gallant J.C.: *Digital terrain analysis*. [in:] Wilson J.P., Gallant J.C. (eds.), *Terrain Analysis: Principles and Applications*, John Wiley & Sons, 2000, pp. 1–27.

[13] Masini N., Coluzzi R., Lasaponara R.: *On the airborne lidar contribution in archaeology: From site identification to landscape investigation*. [in:] Wang C.-C. (ed.), *Laser Scanning: Theory and Applications*, InTech, 2011, pp. 263–290. https://doi.org/10.5772/14655.

[14] Maliqi E., Penev P., Kelmendi F.: *Creating and analysing the Digital Terrain Model of the Slivovo area using QGIS software*. Geodesy and Cartography, vol. 43(3), 2017, pp. 117–123. https://doi.org/10.3846/20296991.2017.1376445.

[15] Rasmus J.C., Hjelle Ø.: *Multiresolution spline models and their applications in geomorphology*. [in:] Evans I.S., Dikau R., Tokunaga E., Ohmori H., Hirano M. (eds.), *Concepts and Modelling in Geomorphology: International Perspectives*, TERRAPUB, Tokyo 2003, pp. 221–237.

[16] Chen Ch., Li Ya., Cao X., Dai H.: *Smooth surface modeling of DEMs based on a regularized least squares method of thin plate spline*. Mathematical Geosciences, vol. 46(8), 2014, pp. 909–929. https://doi.org/10.1007/s11004-013-9519-5.

[17] Wang Y.G., Zhu C.Q., Wang Z.W.: *A surface model of grid DEM based on Coons surface*. Acta Geodaetica et Cartographica Sinica, vol. 37(2), 2008, pp. 217–222.

[18] Zhang J., Lin X.: *Filtering airborne LiDAR data by embedding smoothness-constrained segmentation in progressive TIN densification*. ISPRS Journal of Photogrammetry and Remote Sensing, vol. 81, 2013, pp. 44–59. https://doi.org/10.1016/j.isprsjprs.2013.04.001.

[19] Ali T.: *Building of robust multi-scale representations of LiDAR-based digital terrain model based on scale-space theory*. Optics and Lasers in Engineering, vol. 48(3), 2010, pp. 316–319. https://doi.org/10.1016/j.optlaseng.2009.11.003.

[20] Ali T., Mehrabian A.: *A novel computational paradigm for creating a Triangular Irregular Network (TIN) from LiDAR data*. Nonlinear Analysis: Theory, Methods & Applications, vol. 71(12), 2009, pp. e624–e629. https://doi.org/10.1016/j.na.2008.11.081.

[21] Linyu G., Xiaoping L., Yingcheng L., Pei L., Xiaofeng S., Huijie L.: *Application of breakline and manual additional points in TIN modeling.* [in:] *International Conference on Geo-Spatial Solutions for Emergency Management and the 50th Anniversary of the Chinese Academy of Surveying and Mapping, 14–16 September 2009, Beijing, China*, vol. XXXVIII-7/C4, 2009, pp. 346–351. https://www.isprs.org/proceedings/xxxviii/7-c4/346_gsem2009.pdf [access: 12.01.2024].

[22] Hu G., Wang Ch., Li S., Dai W., Xiong L., Tang G., Strobl J.: *Using vertices of a triangular irregular network to calculate slope and aspect*. International Journal of Geographical Information Science, vol. 36(2), 2022, pp. 382–404. https://doi.org/10.1080/13658816.2021.1933493.

[23] Mingwei Z., Wang J.: *A new method of feature line integration for construction of DEM in discontinuous topographic terrain*. Environmental Earth Sciences, vol. 81, 2022, 387. https://doi.org/10.1007/s12665-022-10527-1.

[24] Zhou Q., Chen Yu.: *Generalization of DEM for terrain analysis using a compound method*. ISPRS Journal of Photogrammetry and Remote Sensing, vol. 66(2), 2011, pp. 38–45. https://doi.org/10.1016/j.isprsjprs.2010.08.005.

[25] Liu X., Che W., Wang Ch.: *Research on a correction method to existing grid-based DEM*. The International Archives of the Photogrammetry, Remote Sensing and Spatial Information Sciences, vol. 37(B1), 2008, pp. 1165–1170.

[26] Bogaert P., Delincé J., Kay S.: *Assessing the error of polygonal area measurements: A general formulation with applications to agriculture*. Measurement Science and Technology, vol. 16(5), 2005, 1170. https://doi.org/10.1088/0957-0233/16/5/017.

[27] Bykat A.: *Automatic generation of triangular grid: I – subdivision of a general polygon into convex subregions. II – triangulation of convex polygons*. The International Journal for Numerical Methods in Engineering, vol. 10(6), 1976, pp. 1329-1342. https://doi.org/10.1002/nme.1620100612.

[28] Conde López E., Salete Casino E., Escribano J.F., Ureña A.V.: *Application of finite element method to create a digital elevation model.* Mathematics, vol. 11(6), 2023, 1522. https://doi.org/10.3390/math11061522.

[29] Bathe K.-J.: *Finite Element Method*. [in:] Wah B.W. (ed.), *Wiley Encyclopedia of Computer Science and Engineering*, John Wiley & Sons, 2008. https://doi.org/10.1002/9780470050118.ecse159.

[30] Suchocki C., Wasilewski A.: *Ustalenie optymalnej siatki GRID dla numerycznego modelu klifu zbudowanego z danych pozyskanych z naziemnego skaningu laserowego.* Prace Naukowe Instytutu Gornictwa Politechniki Wrocławskiej. Konferencje, vol. 129(54), 2009, pp. 111–118.

[31] Kienzle S.: *The effect of grid cell size on major terrain derivatives*. https://proceedings.esri.com/library/userconf/proc04/docs/pap1606.pdf [access: 20.06.2024].

[32] de Aguiar L.A., Guimaraes M.B., Monteiro D.K., da Costa P.D.O.: *Development of a computational routine in Fortran language for analysis of plane and space trusses using the finite element method*. [in:] *CILAMCE 2022: Proceedings of the XLIII Ibero-Latin-American Congress on Computational Methods in Engineering, 21–25 November 2022, ABMEC Foz do Iguaçu – PR – Brazil, Brazil*. http://surl.li/tkxsn [access: 30.04.2024].

[33] Massey P.: *Admissible subspaces and the subspace iteration method*. BIT Numerical Mathematics, vol. 64, 2024, 12. https://doi.org/10.1007/s10543-024-01012-1.

[34] Mayer H.: *Object extraction for digital photogrammetric workstations*. The International Archives of the Photogrammetry, Remote Sensing and Spatial Information Sciences, vol. 35(B2), 2004, pp. 165–173.

[35] Ferreira Z.: *Global and local processes influencing altimetric error patterns in digital elevation models (DEM): An approach on vertical accuracy assessment and spatial aspects of DEM error*. 2024. https://doi.org/10.13140/RG.2.2.14037.84964.

[36] Kim J., Lee S., Seo J., Lee d.e., Choi H.: *The integration of earthwork design review and planning using UAV-based point cloud and BIM*. Applied Sciences, vol. 11, 2021, 3435. https://doi.org/10.3390/app11083435.

[37] Szypuła B.: *DEM from topographic maps – as good as DEM from LiDAR?* [in:] Alvioli M., Marchesini I., Melelli L., Guth P. (eds.), *Proceedings of the Geomorphometry 2020 Conference*, CNR Edizioni, Perugia, Italy, 2020, pp. 119–123. https://doi.org/10.30437/GEOMORPHOMETRY2020_34.

[38] Burke W., Morgan S., Namonje-Kapembwa T., Muyanga M., Mason N.: *Beyond the "Inverse Relationship": Area mismeasurement may affect actual productivity, not just how we understand it.* Agricultural Economics, vol. 54(4), 2023, pp. 557–569. https://doi.org/10.1111/agec.12775.

[39] Holden S., Fisher M.: *Can area measurement error explain the inverse farm size productivity relationship?* Centre for Land Tenure Studies Working Paper, no. 12/13, Norwegian University of Life Sciences (NMBU), Centre for Land Tenure Studies (CLTS), 2013. https://www.econstor.eu/handle/10419/242719 [access: 16.03.2024].

[40] Chen C., Li Y.: *An orthogonal least-square-based method for DEM generalization.* International Journal of Geographical Information Science, vol. 27(1), 2012, pp. 154–167. https://doi.org/10.1080/13658816.2012.674136.

[41] Garnero G., Godone D.: *Comparisons between different interpolation techniques.* The International Archives of the Photogrammetry, Remote Sensing and Spatial Information Sciences, vol. XL-5/W3, 2013, pp. 139–144. https://doi.org/10.5194/isprsarchives-XL-5-W3-139-2013.

[42] de Kok T., van Kreveld M., Löffler M.: *Generating realistic terrains with higher-order Delaunay triangulations.* Computational Geometry, vol. 36(1), 2007, pp. 52–65. https://doi.org/10.1016/j.comgeo.2005.09.005.

[43] Gudmundsson J., Haverkort H.J., van Kreveld M.: *Constrained higher order Delaunay triangulations.* Computational Geometry, vol. 30(3), 2005, pp. 271–277. https://doi.org/10.1016/j.comgeo.2004.11.001.